

An Electrostatic Lens to Reduce Parallax in Banana Gas Detectors.

P. Van Esch
J-F. Clergeau
K. Medjoubi

November 19, 2018

Abstract

Cylindrical "banana" gas detectors are often used in fixed-target experiments, because they are free of parallax effects in the equatorial plane. However, there is a growing demand to increase the height of these detectors in order to be more efficient or to cover more solid angle, and hence a parallax effect starts to limit the resolution in that direction. In this paper we propose a hardware correction for this problem which reduces the parallax error thanks to an applied potential on the front window that makes the electrostatic field lines radially pointing to the interaction point at the entrance window. A detailed analytical analysis of the solution is also presented.

1 Introduction

So-called "banana" detectors are large-area, one-dimensional or 2-dimensional detectors that have a concave cylindrical detection surface. The axis of the cylinder passes through the sample position, and the detector is used to measure the ϕ angle of scattered radiation from the sample in the case of a one-dimensional detector, or to measure ϕ and z in a two-dimensional detector. The advantage of also measuring z is that, in the case of anisotropic samples, one can extract θ information, or in the case of isotropic samples, one can correct for the projection of the cone with opening angle ϕ projected onto a cylindrical surface. Increasing the z -aperture of the detector increases of course the counting efficiency in the case of isotropic samples, and the spherical angle covered in the case of anisotropic samples.

If the detecting volume has a non-negligible thickness, as is often the case for gas detectors, ideally, along the radial line (pointing towards the sample) any detection should give rise to an equivalent "position" detection, which is actually a radial direction detection. In gas detectors, this is a priori not so: the drift field in the detection volume is usually perpendicular to the cylindrical wall, so there will be a dependence of the measured z -value on the exact detection point

along the particle path (a radial line). In the case of neutral particle detection, the distance inside the detection volume of the detection point along the path is usually a random variable with an exponential distribution. A very narrow beam along a well-defined angle θ will give rise to a spread in z -values. This loss in resolution, together with a change of center of gravity of the impact distribution, is called the parallax effect.

The way to avoid this parallax error is to have the electrostatic drift field be radial until the final signal generation. Of course, within a cylindrical geometry, this will not be possible if the final signal generating (gas amplification) surface is equipotential: there the field lines will have to be perpendicular to the cylindrical surface. But one can try to establish at least in the first part of the drift volume a more or less radial electric drift field. A review of parallax correction techniques is given in [1]. A straightforward method is to use a curved entrance window at constant potential, as done by the authors of [2] and [3]. The problem with this approach is of course that the conversion gap changes considerably over the z -range and it is application-dependent if this is acceptable or not. We have been inspired more by the technique described in [4] and [5], to turn the parallel drift field into a radial drift field, at least in the first part of the drift volume. Given the structure of the ‘banana’ detector, we only wish to deflect the field in the z -direction. It turns out that, provided one can make a few approximations, this problem leads to an analytic solution for the potential to be applied at the entrance window.

2 Analytical solution.

We are looking for a potential function $V(z)$, to be applied at the entrance window, such that the E-field is pointing to the sample position at the entrance window. We assume the conversion gap d to be much smaller than the sample distance R . As such we make the following approximation: we assume that the normal component of the electric field E_n is independent of the coordinate ρ (measured perpendicularly on the cylinder surface inward the detection volume) between the entrance window and the detection plane (supposed to be at an equivalent constant potential V_c). Note that we don’t assume that the normal component is independent of z . This is a priori justified by the smallness of the gap compared to all other potential variations which should be of the order of the sample distance. This results in our first equation:

$$E_n(z) = \frac{V(z) - V_c}{d} \quad (1)$$

Next, we want the E-field to be radial at the entrance window, leading to our second equation:

$$\frac{E_t(z)}{E_n(z)} = \frac{z}{R} \quad (2)$$

In this equation, $E_t(z)$ is the tangent component of the E-field at the entrance window. It is determined by the potential gradient:

$$E_t(z) = -\frac{dV}{dz} \quad (3)$$

Note that equations 2 and 3 are exact; our only approximation is equation 1 which we justified, and which we will verify later. The three equations give rise to a linear differential equation in $V(z)$. Solving this equation with the boundary condition that at height h , the potential $V(z)$ has to vanish (the cage is supposed to be at ground potential), we find:

$$V(z) = V_c \left(1 - e^{-\frac{h^2 - z^2}{2Rd}}\right) \quad (4)$$

which is nothing else but a Gaussian profile. To apply such a profile, a suitable sheet (Kapton, for instance) with straight metallic strips, connected by a resistive voltage divider, can be applied. If the strips are regularly spaced at a distance Δ , then of course the resistor values should be chosen as:

$$r_k = r [V(k\Delta) - V((k-1)\Delta)] \quad (5)$$

where r_k is the resistor linking the k -th strip to the previous one, starting from the strip in the middle (at $z = 0$). r is an arbitrary overall scale factor for the resistors, which will determine the total resistance of the voltage divider.

3 Field and drift line calculation.

We apply the above potential in a specific example, namely the geometry for the future D19 banana thermal neutron detector at the ILL: an active height of 40cm ($h = 20cm$), a conversion gap of $d = 2.6cm$ and a sample distance of $R = 70cm$. There are 4cm of extra space on top and at the bottom in the z direction: the entrance window will continue to be at ground potential over these 4cm on each side, as well as the top cover and the bottom cover. The detection "plane" actually consists of a layer of cathode wires at 26 mm from the entrance window, and a layer of anode wires at 30 mm from the entrance window. We will consider the cathode wire plane to be an equipotential surface, and with the applied potentials on the wires, this comes down to an equivalent potential of $V_c = 600V$.

Using a 1mm \times 1mm grid of points in the rectangular drift volume, and applying the relaxation method as explained on p47 of [6], iterating 3000 times yields an accuracy of better than 30mV. The solution for the potential can be seen in figure 1. One can check that the original goal set forth, namely that the electric field at the level of the entrance window points towards the sample position, is satisfied to a high degree, as shown in figure 2, which justifies our approximation after the fact.

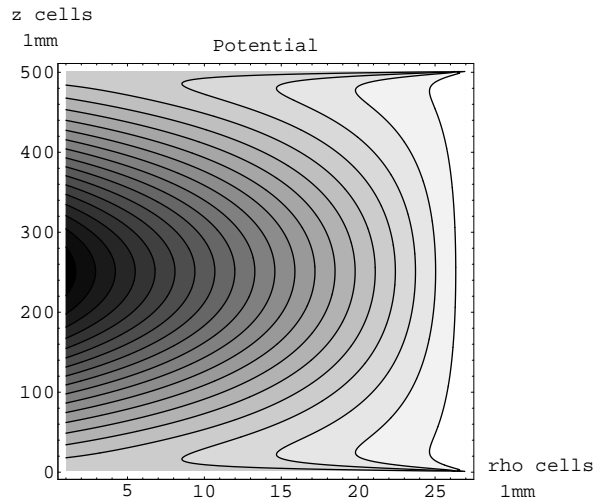


Figure 1: The potential, solved by the relaxation method.

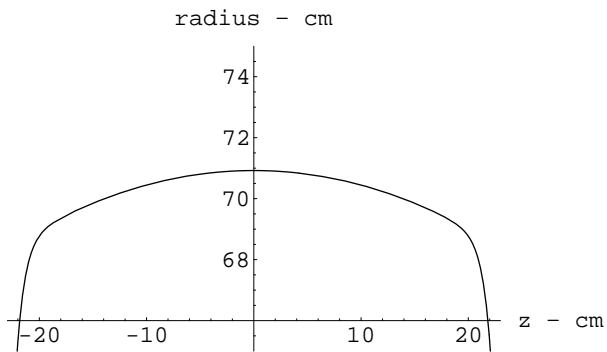


Figure 2: The intersection point of the tangent to the drift line at the entrance window and the central axis. Ideally, this should be equal to the sample distance of 70cm everywhere.

This solution comes close to the following analytical expression:

$$V_{an}(z, \rho) = V_c \frac{d + (\rho - d)e^{\frac{b^2 - z^2}{2Rd}}}{d} \quad (6)$$

On the entrance window and on the detection surface, the expression is exact, and we have a linear interpolation perpendicular to the entrance window. This is another way of stating our approximation as given in equation 1. Clearly, this analytical expression is not a harmonic function and hence cannot be the true solution, but when we take the difference between the numerical values given by this expression and the values found by the relaxation technique, the difference is less than $7.0V$ (maximum error in the middle of the drift volume), which is on the 1% level. The advantage of such a simple expression over numerical results is that solving for the drift lines is possible analytically. Indeed, working out the differential equation for the drift line $z(\rho)$ as a function of the condition $z(\rho_0) = z_0$ gives us the solution:

$$z(\rho) = z_0 \exp\left(\frac{(2d - \rho - \rho_0)(\rho - \rho_0)}{2dR}\right) \quad (7)$$

According to this curve, a neutron that converts in position (z_1, ρ_1) is projected onto the z -value:

$$z_{pr}(z_1, \rho_1) = z_1 \exp\left(\frac{(d - \rho_1)^2}{2dR}\right) \quad (8)$$

Clearly without the electrostatic lens, the exponential factor is absent.

4 Projected image of a ray.

We consider an incident beam from the sample position under an angle θ . After having travelled a distance s in the conversion gap, the particle is at position $(\rho_1 = \cos \theta s, z_1 = R \tan \theta + \sin \theta s)$. The ray will thus give rise to hits which are confined between $Re^{\frac{d}{2R}} \tan \theta \simeq (R + \frac{d}{2}) \tan \theta$ and $(R + d) \tan \theta$. Without lens, this ray would give rise to hits between $R \tan \theta$ and $(R + d) \tan \theta$, which means that the carrier of the hit distribution with lens is divided by 2 as compared to without a lens. But in order to work out more accurately the improvement upon the parallax error, we need to work out the projected conversion density.

If we consider an absorption (conversion) constant μ , the projected density $\xi_\theta(z)$ of a narrow beam emanating from the sample under an angle θ can be found by working out:

$$\xi_\theta(z) = \int_{s=0}^{s_{max}} \mu e^{-\mu s} \delta\left[z - (R \tan \theta + s \sin \theta) \exp\left(\frac{(d - s \cos \theta)^2}{2dR}\right)\right] ds \quad (9)$$

with $s_{max} = d/\cos \theta$. In order to solve this integral, we need to know $s_0(z, \theta)$, the solution to the equation:

$$(R \tan \theta + s_0 \sin \theta) \exp\left(\frac{(d - s_0 \cos \theta)^2}{2dR}\right) = z \quad (10)$$

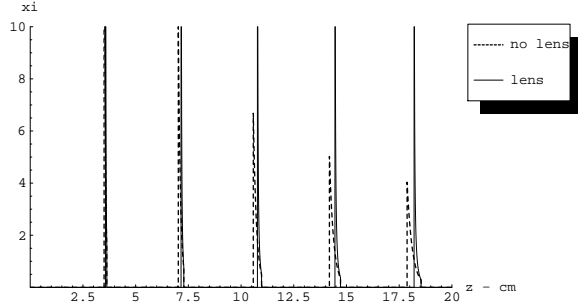


Figure 3: The projected densities, with and without lens, for $\mu = 1\text{cm}^{-1}$. The represented beams have angles 0.05,0.1,0.15,0.20 and 0.25 rad.

As such, this equation cannot be solved analytically. However, noting that $d/R \ll 1$, we can expand the exponential term, and limit ourselves to first-order contributions in d/R . This approximate solution is given as follows:

$$s_0(z, \theta) \simeq \sqrt{d} \sqrt{\csc \theta} \sqrt{\sec \theta} \sqrt{2z - (d + 2R) \tan \theta} \quad (11)$$

If $s_0(z, \theta)$ is between 0 and s_{max} , which comes down to requiring that z is within the limits of the carrier of ξ_θ , we finally find for the projected density of a ray under the effect of the lens:

$$\xi_\theta(z) = \frac{2dR \csc \theta \mu e^{-\mu s_0(z, \theta)}}{d^2 + 2(-2d + R) \sqrt{d} \cot \theta \sqrt{2z - (d + 2R) \tan \theta}} \quad (12)$$

Without the lens, the projected density is given by:

$$\xi_\theta^0(z) = \int_{s=0}^{s_{max}} \mu e^{-\mu s} \delta[z - (R \tan \theta + s \sin \theta)] ds \quad (13)$$

which has as a solution:

$$\xi_\theta^0(z) = \mu \exp\left(-\mu \left(\frac{z}{\sin \theta} - \frac{R}{\cos \theta}\right)\right) \frac{1}{\sin \theta} \quad (14)$$

where it is understood that z is within the boundaries of the carrier of ξ_θ^0 .

5 Resolution improvement: an example.

We will now take as an example the case $\mu = 1\text{cm}^{-1}$, and the geometry of the D19 prototype detector described earlier. If we compare the projected densities for different beams, we obtain profiles as shown in figure 3.

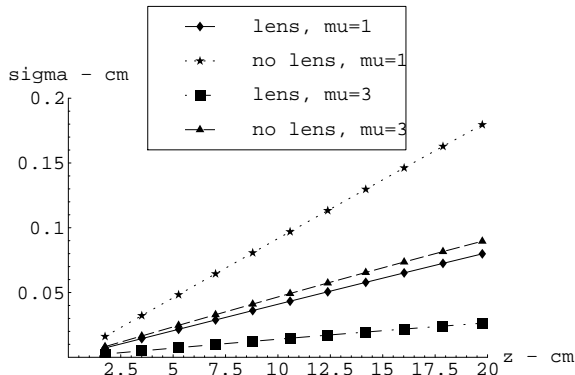


Figure 4: Resolution (standard deviation of projected density) as a function of the impact position at the front window, for the cases $\mu = 1\text{cm}^{-1}$ and $\mu = 3\text{cm}^{-1}$, at a fixed impact angle $\theta = 0.275$.

We calculate the standard deviations of these distributions by numerical integration, and also of the distributions obtained with $\mu = 3.0\text{cm}^{-1}$. We obtain the result shown in figure 4. The resolutions are improved using a lens by a factor slightly better than 2.2 for the case $\mu = 1\text{cm}^{-1}$ and a factor slightly better than 3.3 for $\mu = 3\text{cm}^{-1}$. If we double the conversion gap (from 2.6 mm to 5.2 mm), and we do the calculation again, we find that for $\mu = 1\text{cm}^{-1}$ the improvement is a factor of about 2.6 and for $\mu = 3\text{cm}^{-1}$ the improvement is even a factor of about 5.5. This means that the relative improvement of the resolution error due to parallax increases as well when d as well as when μ become large. However, we should pay attention to the absolute resolutions as a function of thickness. In figure 5, we can observe that the resolution without lens has a saturating behavior as a function of conversion gap thickness, while the behavior with lens is better, but more involved, in that the resolution reaches a maximum, and then decreases when the conversion gap gets bigger.

Experimentally, the prototype has been filled with 5.5 bar of He-3. Neutrons with a wavelength of 2.5 Angstrom are used, which comes down to a conversion factor $\mu = 0.99\text{cm}^{-1}$. A Cd mask with 2 mm wide slits was put in front of the entrance window, and a piece of plexiglass irradiated at the sample position diffused the narrow neutron beam in a more or less radially uniform way. Activating or not, the electrostatic lens, we obtain the resolutions, obtained by fitting a gaussian curve with offset to the slit images using a least-squares algorithm, as shown in figure 6. The resolution finds its origin in several different effects (intrinsic gas resolution, electronic noise, quantization noise,...), but the deterioration due to parallax is clearly visible, and is improved upon by the lens action.

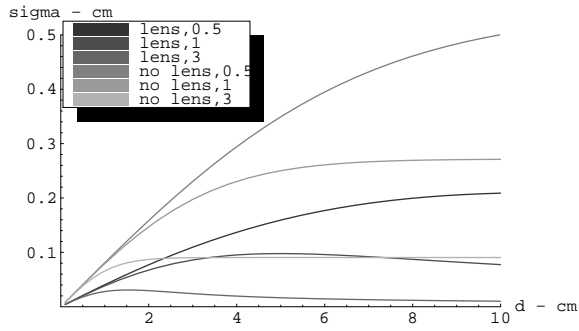


Figure 5: Resolution (standard deviation of projected density) as a function of the thickness of the conversion volume, for the cases $\mu = 0.5\text{cm}^{-1}$, $\mu = 1\text{cm}^{-1}$ and $\mu = 3\text{cm}^{-1}$.

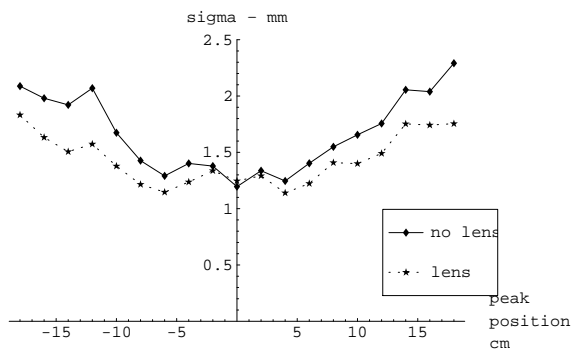


Figure 6: The measured resolution (standard deviations of a gaussian fit in mm) as a function of impact position.

6 Conclusion

A solution has been presented to improve upon the parallax effect in large-aperture banana detectors, using an electrostatic lens. An approximate analytical expression of the expected image of a ray is deduced. Calculations indicate that the relative improvement upon the parallax error with this method becomes stronger when both μ and d are large. The absolute resolution, with lens, has a more complicated behavior as a function of d . An experimental verification of the improvement, using the prototype of the new D19 thermal neutron detector at the ILL, indicates qualitatively that the technique works in practice.

References

- [1] G. Charpak, Nucl. Instr. Meth. 201 (1982), 181-192.
- [2] Yu.V. Zanevsky, S.P. Chernenko et *al.*, Nucl. Instr. Meth. A 367 (1995) 76-78
- [3] Yu.V. Zanevsky, S.P. Chernenko et *al.*, Nucl. Phys. B 44 (1995) 406-408
- [4] V. Comparat et al, French patent n 2 630 829 (1988).
- [5] P. Rehak, G.C. Smith and B. Yu, IEEE Trans. Nucl. Sci., vol 44, no. 3 (1997) 651-655.
- [6] J. D. Jackson, Classical Electrodynamics, third edition, ©John Wiley 1999.